

This article was downloaded by:

On: 15 January 2011

Access details: *Access Details: Free Access*

Publisher *Taylor & Francis*

Informa Ltd Registered in England and Wales Registered Number: 1072954 Registered office: Mortimer House, 37-41 Mortimer Street, London W1T 3JH, UK



## Journal of Experimental Nanoscience

Publication details, including instructions for authors and subscription information:

<http://www.informaworld.com/smpp/title~content=t716100757>

### Biofunctionalised quantum dots for sensing and identification of waterborne bacterial pathogens

Sonal Mazumder<sup>a</sup>; Jhimli Sarkar<sup>a</sup>; Rajib Dey<sup>b</sup>; M. K. Mitra<sup>b</sup>; S. Mukherjee<sup>b</sup>; G. C. Das<sup>b</sup>

<sup>a</sup> School of Materials Science & Nanotechnology, Jadavpur University, Kolkata 700032, West Bengal, India <sup>b</sup> Department of Metallurgical and Material Engineering, Jadavpur University, Kolkata 700032, West Bengal, India

Online publication date: 05 November 2010

**To cite this Article** Mazumder, Sonal , Sarkar, Jhimli , Dey, Rajib , Mitra, M. K. , Mukherjee, S. and Das, G. C.(2010) 'Biofunctionalised quantum dots for sensing and identification of waterborne bacterial pathogens', *Journal of Experimental Nanoscience*, 5: 5, 438 – 446

**To link to this Article:** DOI: 10.1080/17458081003588010

URL: <http://dx.doi.org/10.1080/17458081003588010>

PLEASE SCROLL DOWN FOR ARTICLE

Full terms and conditions of use: <http://www.informaworld.com/terms-and-conditions-of-access.pdf>

This article may be used for research, teaching and private study purposes. Any substantial or systematic reproduction, re-distribution, re-selling, loan or sub-licensing, systematic supply or distribution in any form to anyone is expressly forbidden.

The publisher does not give any warranty express or implied or make any representation that the contents will be complete or accurate or up to date. The accuracy of any instructions, formulae and drug doses should be independently verified with primary sources. The publisher shall not be liable for any loss, actions, claims, proceedings, demand or costs or damages whatsoever or howsoever caused arising directly or indirectly in connection with or arising out of the use of this material.

## Biofunctionalised quantum dots for sensing and identification of waterborne bacterial pathogens

Sonal Mazumder<sup>a</sup>, Jhimli Sarkar<sup>a</sup>, Rajib Dey<sup>b\*</sup>, M.K. Mitra<sup>b</sup>, S. Mukherjee<sup>b</sup> and G.C. Das<sup>b</sup>

<sup>a</sup>School of Materials Science & Nanotechnology, Jadavpur University, Kolkata 700032, West Bengal, India; <sup>b</sup>Department of Metallurgical and Material Engineering, Jadavpur University, Kolkata 700032, West Bengal, India

(Received 8 September 2009; final version received 28 December 2009)

Harmful bacteria are the most common cause of food- and waterborne illnesses. Infection often leads to bloody diarrhoea, and occasionally to kidney failure. Several strains of the bacteria *Escherichia coli* produce a powerful toxin which causes serious illness. Food and water can be contaminated with other bacteria like Salmonella, Coliform, Pseudomonas, etc. Hence, it has become important to rapidly detect and identify infectious bacteria. Colloidal luminescent semiconductor nanocrystals or quantum dots (QDs) have elicited a great deal of interest in the biosensing community due to their unique fluorescent properties. Here ZnS:Mn<sup>2+</sup> QDs are synthesised and biofunctionalised with chitosan. They are attached to the anionic cell wall of *E. coli* bacteria and different properties of this compound system are studied. These nanocrystals may offer cost effective and quicker alternative to detect single bacterium compared to other conventional methods. The process of the synthesis of QDs, biofunctionalisation and detection of bacteria have been characterised by XRD, UV-Vis spectroscopy, FTIR, photoluminescence spectroscopy, AFM, high-resolution transmission electron microscopy and confocal microscopy. The particle size calculated is approximately 8–10 nm. The blue shift of PL peak has been observed after the bacteria get attached.

**Keywords:** quantum dots; biological labelling; identification; waterborne bacteria; chitosan; spectral shift

### 1. Introduction

*Escherichia coli* has the ability to produce a toxin causing serious gastrointestinal infections that are responsible for different diseases like hemorrhagic colitis and hemolytic uremic syndrome. Some other waterborne bacteria like *Clostridium botulinum*, *Mycobacterium marinum*, *Shigella* sp. and *Salmonella typhi* cause diseases like botulism, chronic glaucomatous, shigellosis and typhoid, respectively [1].

---

\*Corresponding author. Email: rajib.dey@gmail.com

The different conventional methods used to detect bacteria are listed below along with their limitations [2].

Sl. no.	Conventional methods to detect bacteria	Limitations
1	Culture techniques	Time consuming
2	Polymerase chain reaction (PCR) analysis	Lack of sensitivity
3	Enzyme-linked immunosorbent assays (ELISAs)	Lack of specificity
4	Fluorescence-based assays	Stability needed for rapid diagnosis

Semiconductor nanocrystals or quantum dots (QD), extremely small in size, exhibit properties attributed to the quantum effect. They are highly photostable with broad absorption spectra and narrow size tuneable emission spectra. The size and shape of their structure and the number of electrons they contain can be precisely controlled. Unlike the organic dye, which has the disadvantage of a bleaching effect, QDs continue to emit a non-decaying signal even with repeated cycles of light excitation. Thus, when QDs are coupled to biomolecules, intracellular processes can be monitored over a prolonged period. The colour of QDs can be adjusted by varying the size of nanocrystals [3–7].

More often than not, the main challenge in using QDs in biological applications lies in the QDs, which as synthesised, have a layer of hydrophobic organic ligands on their surface [8–12]. Most of the synthesis methods that produce highly monodisperse, homogeneous nanoparticles use organic solvents. But the particles that are produced need to be rendered water soluble for biological applications. In order to render the QDs water soluble, these organophilic surface species are generally exchanged for species that are more polar. However, QDs capped with these small molecules are easily degraded by hydrolysis or oxidation of the capping ligands. To overcome these problems, different polymerisation techniques for incorporating QDs into polymer micro beads have been used and reported. Chitosan, a natural biopolymer obtained by the alkaline deacetylation of chitin, is hydrophilic, nontoxic, biocompatible and biodegradable [13,14].

Furthermore, biodistribution of chitosan-capped nanoparticles and the mechanism of their delivery to cells and tissues remain unclear. It is noted that chitosan molecules contain amino groups, which can be used as active reaction sites to be linked to the carboxylic-functionalised QDs [11,12]. In this work, luminescent chitosan-capped nanoparticles embedded with QDs were synthesised. These nanoparticles will be useful for either various bioassays or intracellular labelling.

Manganese (Mn)-doped zinc sulphide QDs have been synthesised and used for labelling different biomolecules. But there is hardly any literature that supports the detection and identification of bacteria by QDs. Therefore, it would be worthwhile to explore the possibility of attaching the chitosan-capped QDs to the surface of the pathogenic bacteria to detect the minute amount of contamination in the sample. It is useful for the detection of bacteria that are not easy to culture using a much simpler and cost effective process.

## 2. Experimental materials and method

Mn<sup>2+</sup>-doped QDs (ZnS:Mn<sup>2+</sup>) were prepared by a chemical route using a suitable biocompatible capping agent. This method is similar to that described by Bhargava et al. [14]

with a suitable modification. ZnS is used as it is less toxic compared to other elements like Cd, etc. Mn doping is done in order to passivate the ZnS and consequently its high luminescence occurs at around 600 nm [15]. Chitosan is a biocompatible capping agent and also prohibits the diffusion of ions from the solution and restricts the growth of QD. It is also nontoxic, hydrophilic and biodegradable.

A 0.25 M zinc acetate and 2 % Mn acetate are mixed together along with 0.1–0.2% chitosan and constantly stirred in a magnetic stirrer for nearly 20 min. The solution was then heated to 80°C for about half an hour. After cooling to room temperature, the sample was kept in ice bath and 0.25 M sodium sulphide solution was added dropwise with constant stirring with a glass rod with the formation of white precipitate of ZnS nanoparticles immediately. The supernatant was then centrifuged at 3500 rpm for 40 min to sediment-agglomerated particles. The sample was then freeze-dried for nearly 18 h and a papery material was obtained. Then the sample was kept in a desiccator for few days followed by grinding. Coliform bacteria were cultured. The strain used for this purpose was *E. coli* (ATCC 25922).

The sample has been thoroughly characterised by using UV-Vis spectroscopy (Perkin-Elmer, Lambda 35) to measure the transmission and absorption spectra. Photoluminescence measurement has been carried out with ZnS:Mn<sup>2+</sup> powder at room temperature using glass substrates (Spectra Physics). X-ray diffraction patterns of these samples were taken with Cu-K $\alpha$  radiation (Rigaku, Ultima III). Surface morphology of the sample was analysed using 3  $\times$  3  $\mu$ m probe of atomic force microscopy (NTMDT) and high-resolution transmission electron microscopy (HRTEM) (JEOL, JEM 2100). The samples were further characterised by FTIR spectroscopy (Prestige 22, Shimadzu) and confocal microscopy (Zeiss LSM 510).

### 3. Results and discussion

#### 3.1. UV-Vis spectroscopy

Figure 1 represents a typical transmittance spectrum of QDs dispersed in water over the range of 500–200 nm. The figure shows a sharp absorption edge at 239 nm, characteristic of crystalline nature of these QDs. The crystalline nature of the QDs has further been substantiated by the presence of XRD peaks (Figure 2). The band gap from this absorption edge that has been calculated using the standard technique and is

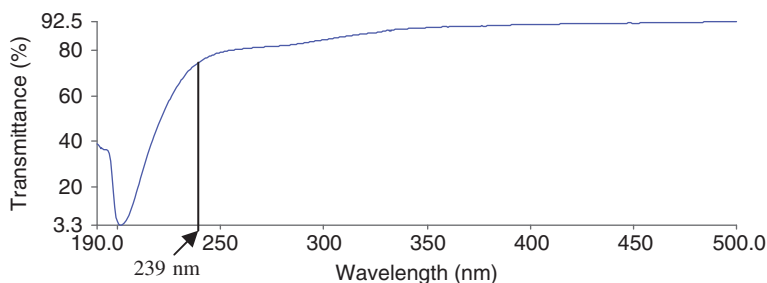


Figure 1. Transmittance spectrum of the QD sample.

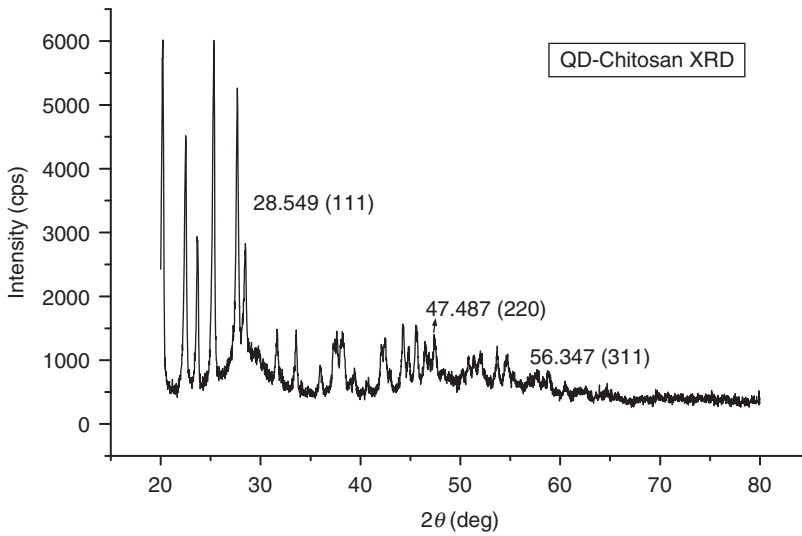


Figure 2. The X-ray diffraction pattern of ZnS: Mn<sup>2+</sup> QD capped with chitosan.

found to be 5.21 eV. The bulk band gap value of ZnS is 3.68 eV [16]. This implies an increase in the band gap ( $\Delta E_g$ ) by 1.53 eV in the Mn-doped QD samples.

This increase in the band gap is used to compute the size of QDs using [16,17].

$$\Delta E_g = E_g(\text{powder}) - E_g(\text{bulk}) = (h^2/8\mu r^2) - (1.8e^2/\epsilon r), \tag{1}$$

where  $h$  = Planck's constant,  $\epsilon$  = dielectric constant,  $e$  is the electronic charge,  $r$  is the size of the QD and  $\mu$  is the reduced mass defined by,

$$\mu = m_e^* m_h^* / m_e^* + m_h^*,$$

where  $m_e^*$  = effective mass of electrons and  $m_h^*$  = effective mass of holes.

The computed size of the QD is found to be 1.1 nm.

### 3.2. X-ray diffraction (XRD)

Figure 2 represents a typical XRD pattern of ZnS:Mn<sup>2+</sup> capped with chitosan. The diffractogram shows the presence of strong peaks of Mn<sub>0.1</sub>Zn<sub>0.9</sub>S. Using the Scherrer formula we get the average computed size of QD as 11 nm. The size is found to be larger than that found from the UV-Vis transmittance spectrum. This is possibly because the particles suspended in water used for taking UV-Vis spectrum are more dispersed compared to that of solid powder samples used for XRD.

### 3.3. Fourier transforms infrared (FTIR) spectroscopy

The IR spectrum of pure chitosan (Figure 3(a)) shows that the intensities of the absorbances at 1650 and 1560 cm<sup>-1</sup>, corresponding to amide I and amide II bands,

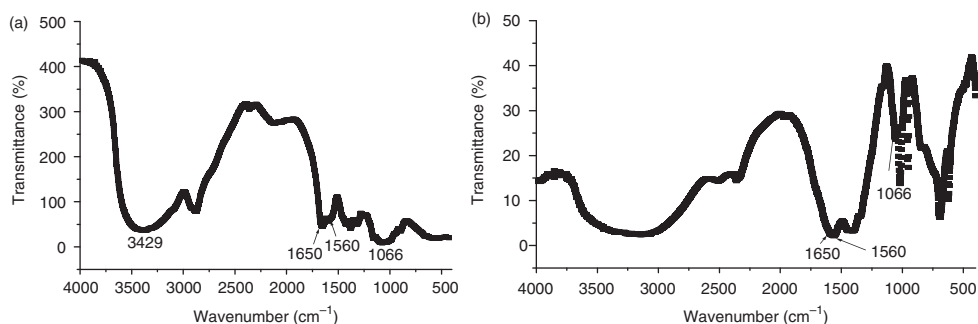


Figure 3. FTIR of (a) chitosan polymer and (b) ZnS: Mn<sup>2+</sup> along with chitosan capping.

respectively, are lower than that at  $1066\text{ cm}^{-1}$  assigned to  $-\text{C}-\text{O}-\text{C}-$  vibration [18]. However, the reverse result was observed for chitosan-capped nanoparticles, i.e. the absorbances at  $1650$  and  $1560\text{ cm}^{-1}$  are stronger than that at  $1066\text{ cm}^{-1}$  (Figure 3(b)).

### 3.4. Atomic force microscopy (AFM)

Figure 4(a) shows a typical surface morphology of chitosan-capped QD as revealed by AFM, which clearly shows the distribution of the particle size. Figure 4(b) shows the particle size distribution over the range 4–10 nm with maximum frequency for particle size at 7 nm, which agrees with the order of magnitude of the particle size (11 nm) predicted by XRD. But the size of the QDs produced by UV-Vis is distinctly lower ( $\approx 1$  nm), which may probably be due to dispersion of QDs in water used for taking UV-Vis spectra (Figure 1), as mentioned earlier.

### 3.5. Transmission electron microscopy (TEM)

Figure 5 shows an HRTEM image of chitosan-encapsulated QDs taken by GATTAN CCD. It clearly shows that chitosan of the order of a few tens of nanometre encapsulate Mn-doped ZnS nanocrystals of a few nanometre in size (dark globular). This compares reasonably well with the particle size obtained from the UV-Vis measurement. This is because in either measurement the sample is prepared by the dispersion of QDs in aqueous medium. The inset shows the selected area diffraction pattern taken on GATTAN CCD. The calculated  $d$  values from SAED pattern corroborates the  $d$ -values obtained from XRD. This further indicates the presence of the Mn-doped ZnS nanoparticles.

### 3.6. Confocal microscopy

A slide was prepared where bacteria were heat fixed and QD powders were sprinkled. The slide was incubated for sometime and then rinsed several times to remove the unattached nanoparticles. Under confocal microscope, in some parts of the slide, green fluorescence has been clearly observed (Figure 6). This arises due to the attachment of QD to bacteria. This has further been substantiated by photoluminescence spectral study.

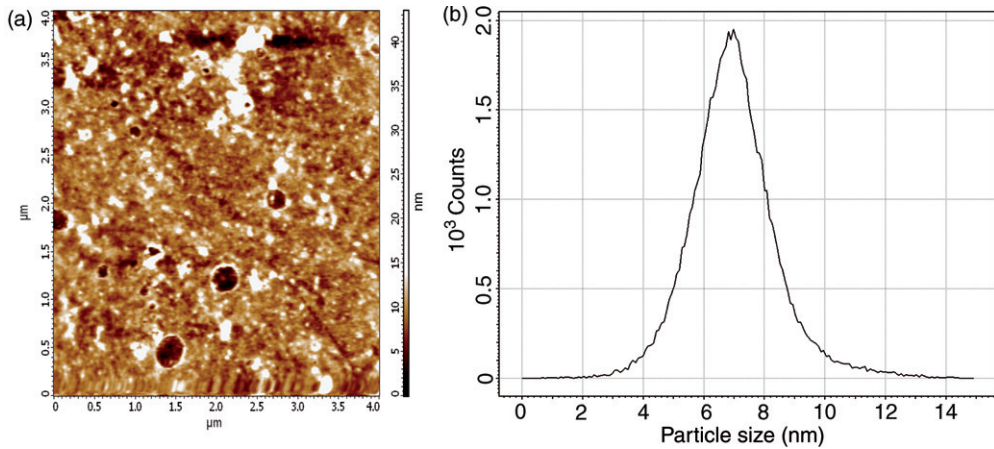


Figure 4. (a) AFM of chitosan-capped QD and (b) particle size distribution.

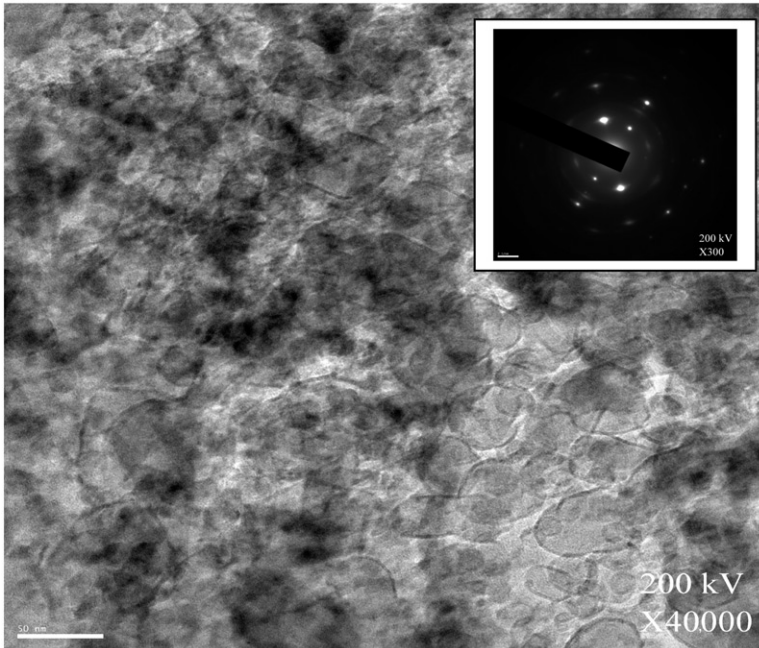


Figure 5. TEM image of chitosan-encapsulated QD nanoparticles. Inset is the SAED image.

### 3.7. Photoluminescence spectroscopy (PL)

The photoluminescence spectra have been recorded corresponding to the excitation wavelength of 440 nm for chitosan-encapsulated Mn-doped ZnS QDs and the same attached with bacteria and are shown, respectively, in Figure 7(a) and (b). Figure 7(a) shows the characteristic PL peak at 590 nm corresponding to the doped ZnS QDs.

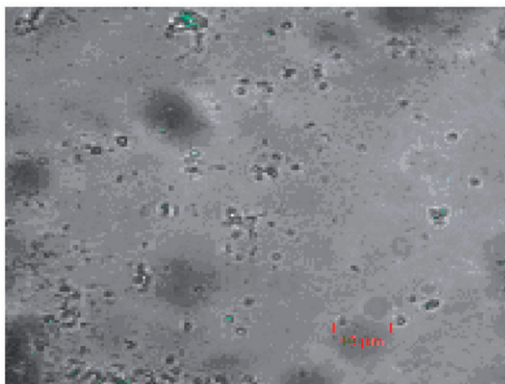


Figure 6. Confocal microscopic image of QD attached to bacteria.

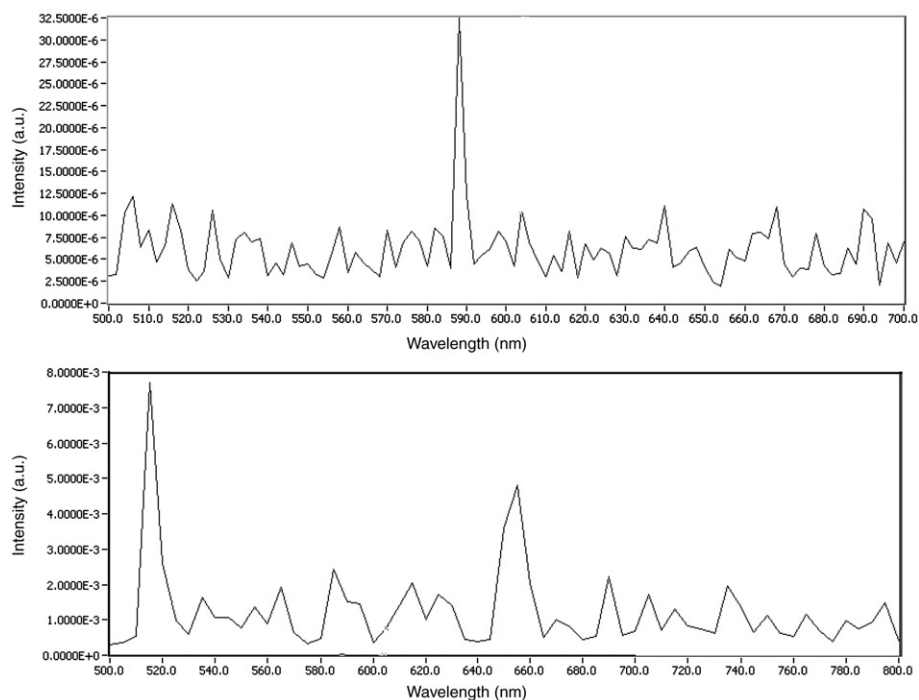


Figure 7. (a) PL spectrum for chitosan-encapsulated Mn-doped ZnS and (b) PL spectrum for chitosan-encapsulated Mn-doped ZnS attached with bacteria.

But when attached with bacteria (Figure 7(b)), the PL peak appears at 520 nm. This distinct blue shift can therefore be utilised as a tool to confirm the attachment of bacteria. Green fluorescence in confocal microscopy corroborates blue shift of PL peak from 590 nm (orange) to 520 nm (green) as chitosan-encapsulated QDs get attached to bacteria (colour online).



#### 4. Conclusions

- ZnS:Mn<sup>2+</sup> QDs were synthesised as revealed from XRD and SAED patterns.
- The size of these crystallites was 1.1 nm as calculated from the UV-Vis transmission spectrum, which agrees fairly well with the image of TEM.
- The size of the QDs encapsulated with chitosan was found to be peaked around 7 nm, as seen from the AFM image which agrees with the order of magnitude of particle size obtained from XRD (11 nm).
- Confocal microscopic image shows that bacteria were attached to the chitosan-encapsulated QDs and the blue shift of the PL peak can be used as a tool to confirm this attachment of bacteria with chitosan-encapsulated QDs.

Hence, chitosan-encapsulated QDs may be easily used as biosensors to mark the presence of bacteria in water, food preservative and other contaminated samples in a few hours which when done by conventional methods, followed by biochemical identification might take a total time assay up to one week.

#### Acknowledgements

The authors acknowledge the help rendered by Mr Poritosh Chakraborty of Food Technology Department and Prof T. Chatterjee and Prof S. Ghosh Dastidar of the Pharmacy Department of Jadavpur University, Kolkata. The authors are grateful to Dr Anuradha Lohia, Bose Institute, Kolkata, for her help in taking confocal microscopic images. The authors also thank Dr Anil Adhikari, Sk Farooq Ahmed, Mr Sudhir Ghosh, Mr Sumon Nandi, Mr Chandan Ghosh, Mr Amitavo Das and Mr Subhranshu Chatterjee of Jadavpur University for helping with different characterisations and experimental processes and express special thanks to UGC-UPE for supporting the work.

#### References

- [1] K.G. Rainis, *Guide to Microlife*, Franklin Watts, New York, 1996.
- [2] M.A. Hahn, J.S. Tabb, and T.D. Krauss, *Detection of single bacterial pathogens with semiconductor quantum dots*, *Anal. Chem.* 77 (2005), pp. 4861–4869.
- [3] X.H. Gao and S.M. Nie, *Quantum dot-encoded mesoporous beads with high brightness and uniformity: Rapid readout using flow cytometry*, *Anal. Chem.* 76 (2004), pp. 2406–2410.
- [4] S.G. Penn, L. He, and M.J. Natan, *Nanoparticles for bioanalysis*, *Curr. Opin. Chem. Biol.* 7 (2003), pp. 609–615.
- [5] K. Braeckmans, S.C. De Smedt, M. Leblans, R. Pauwels, and J. Demeester, *Encoding microcarriers: Present and future technologies*, *Nat. Rev. Drug Discov.* 1 (2002), pp. 447–456.
- [6] D.R. Walt, *Imaging optical sensor arrays*, *Curr. Opin. Chem. Biol.* 6 (2002), pp. 689–695.
- [7] J.A. Ferguson, F.J. Steemers, and D.R. Walt, *High-density fiber-optic DNA random microsphere array*, *Anal. Chem.* 72 (2000), pp. 5618–5624.
- [8] B. Dubertret, P. Skourides, D.J. Norris, V. Noireaux, A.H. Brivanlou, and A. Libchaber, *In vivo imaging of quantum dots encapsulated in phospholipidmicelles*, *Science* 298 (2002), pp. 1759–1762.
- [9] D. Gerion, F. Pinaud, S.C. Williams, W.J. Parak, and D. Zanchet, *Synthesis and properties of biocompatible water-soluble silica-coated CdSe/ZnS semiconductor quantum dots*, *J. Phys. Chem. B* 105 (2001), pp. 8861–8871.

- [10] H. Mattoussi, J.M. Mauro, E.R. Goldman, G.P. Anderson, and V.C. Sundar, *Self-assembly of CdSe–ZnS quantum dot bioconjugates using an engineered recombinant protein*, J. Am. Chem. Soc. 122 (2000), pp. 12142–12150.
- [11] C.B. Murray, D.J. Norris, and M.G. Bawendi, *Synthesis and characterization of nearly monodisperse CdE (E = S, Se, Te) semiconductor nanocrystallites*, J. Am. Chem. Soc. 115 (1993), pp. 8706–8715.
- [12] Y.F. Chen and Z. Rosenzweig, *Luminescent CdSe quantum dot doped stabilized micelles*, Nano Lett. 2 (2002), pp. 1299–1302.
- [13] P. O'Brien, S.S. Cummins, D. Darcy, A. Dearden, O. Masala, N.L. Pickett, S. Ryley, and A.J. Sutherland, *Quantum dot-labelled polymer beads by suspension polymerisation*, Chem. Commun. 13 (2003), pp. 2532–2533.
- [14] R.N. Bhargava, D. Gallagher, X. Hong, and A. Nurmikko, *Optical properties of manganese-doped nanocrystals of ZnS*, Phys. Rev. Lett. 72 (1994), pp. 416–419.
- [15] H.C. Warad, S.C. Ghosh, B. Hemtanona, C. Thanachayanontb, and J. Dutta, *Luminescent nanoparticles of Mn-doped ZnS passivated with sodium hexametaphosphate*, Sci. Technol. Adv. Mater 6 (2005), pp. 296–301.
- [16] R. Maity and K.K. Chattopadhyay, *Synthesis and optical characterization of ZnS and ZnS: Mn nanocrystalline thin films by chemical route*, Nanotechnology 15 (2004), pp. 812–816.
- [17] J.I. Pankove, *Optical Processes in Semiconductors*, Prentice-Hall, Englewood Cliffs, NJ, 1971.
- [18] Q. Nie, W.B. Tan, and Y. Zhang, *Synthesis and characterization of monodisperse chitosan nanoparticles with embedded quantum dots*, Nanotechnology 17 (2006), pp. 140–144.